Mansoura Bulletin Vol. 7, No. 2, December 1982. C.1

NUMERICAL ANALYSIS OF MACHINE ELEMENTS
CASE STUDY OF ACTUAL FAILURE

BY

DR. GALAL ABDEL-HAMID ABDELLAH *

DR. HASSAN M. HOSNY **

(1) INTRODUCTION :

With the ever increasing competition in the industry between different manufacturers in marketing their products , economy in the design of each element of any machine became a must especially for those expensive machines used in heavy industry. In the past,the construction of such machines was mainly depending on the practical experience of each manufacturer. Such an experience was based on simplified analysis of each machine element and or experimental investigations. The resulting design data gained by such methods were not sufficient enough to cover all the design aspects required. Accordingly this might lead to an over or under estimated designs.

The expansion of the use of computers together with the development of numerical methods gave a powerfull tool to analyse the stress conditions in such machine structures. This can help not only in the original design but also in evaluating causes of any deffects which might take place during the life time of the machine.

In the present paper the finite element method is applied on a practical case of periodic failure of a scrap shearing machine. The cause of failure is determined and recommendations for avoiding such failure are given.

(2) DISCRIPTION OF THE PROBLEM :

The machine under consideration fig.[1] is a metal scrap shearing machine with a wide bed , a side press and a pressing cover. The scrap charge is pressed by the side press and the press cover into a block. A push feeder pushes the scrap block under the shearing edge.

* Lecturer,Struct.Eng.Mansoura University,Egypt

** Associate Prof.,Struct.Eng.Dept.Mansoura Univ.,Egypt.

The bracket (diaphragm) ABCDE fig.[2], welded to the press cover and connected to a hydraulic cylinder-providing the required pressure-was subjected to periodic failure along the welded edge AB.

(3) FINITE ELEMENT MODELING :

Due to the nature of the problem under consideration fig. [2] i.e. the non-regular geomtry of the press cover as a thin walled structure,the various boundary conditions and the variable loading conditions,the use of the finite element was thought to be the most suitable method. As the press cover is symmetrical along the bracket axis,it was decided to consider only one half of it in the analysis as a non-prizmatic folded plate structure supported on the bracket ABCDE (as a diaphragm) and hinged along the line BG. Fig.[3] shows the finite element mesh used in the analysis. The bracket was considered as a two dimensional plane stress element supported at nodes 70 and 88 and welded to the press cover along the lines AB,BC,CD and DE. Fig.[4] shows the finite element mesh used in the analysis. As far as the loading conditions are concerned,the two extreme cases shown in fig.[2] were considered. The first case fig.[2a] represents the case where the metal scrap is considered to be lumped under the bracket,resulting the maximum normal stress in the bracket. The second case fig. [2b] represents the case where the metal scrap is lumped at the extreme end of the press cover resulting the maximum edge shearing forces along the lines ABCDE.

(4) ELEMENT USED :

The element used in this analysis,fig.[5] is a refined traingular element with six degrees of freedom per node , i.e.three translations and three rotations,which are assumed to vary independently and linearly over the domain of the element.

The unkown parameters of the assumed displacement functions are determined by the principle of minimum potential energy. The variational principle is applied to each element separately ; thus ;

$$\iint_{(A)} \{\varepsilon\}^T [H_1] \{\delta\varepsilon\} dA + \iint_{(A)} \{\chi\}^T [H_2] \{\delta\chi\} dA + \iint_{(A)} \{\gamma\}^T [H_3] \{\delta\gamma\} dA$$

$$- \sum_{i=1}^{i=3} \{P_m\}_i^T \{\delta d_m\} - \sum_{i=1}^{i=3} \{P_b\}^T \{\delta d_b\} = 0. \quad (1)$$

where

$$\{\varepsilon\}^T = \{ \frac{\partial u}{\partial x} \quad \frac{\partial v}{\partial y} \quad (\frac{\partial u}{\partial y} + \theta_z) \quad (\frac{\partial v}{\partial x} - \theta_z) \}$$

$$\{\chi\}^T = \{ -\frac{\partial \theta_y}{\partial x} \quad \frac{\partial \theta_x}{\partial y} \quad (\frac{\partial \theta_x}{\partial x} - \frac{\partial \theta_y}{\partial y}) \} \quad (2)$$

$$\{\gamma\}^T = \{ (\frac{\partial w}{\partial x} + \theta_y) \quad (\frac{\partial w}{\partial y} - \theta_x) \}$$

represent the strains , while

$$[H_1] = \frac{Eh}{1-v^2} \cdot \begin{bmatrix} 1 & v & 0 & 0 \\ v & 1 & 0 & 0 \\ 0 & 0 & 0 & 1-v \\ 0 & 0 & 1-v & 0 \end{bmatrix} , \quad [H_2] = \frac{Eh}{12(1-v^2)} \cdot \begin{bmatrix} 1 & v & 0 \\ v & 1 & 0 \\ 0 & 0 & (1-v)/2 \end{bmatrix}$$

and

$$[H_3] = \frac{Eh}{2(1+v)} \cdot \begin{bmatrix} 1 & 0 \\ 0 & 1 \end{bmatrix} \quad (3)$$

are the pertinent constitutive matrices that express the Hooke's law.

The variation of the membrane part of the strain energy is given in the first term of Eq.(1),while its second and third terms describe the variation of the strain energy created by bending and shear deformations,respectively. The last two terms express the change of the potentials of the in-plane (P_m) and lateral (P_b) nodal forces.

The displacement fields are expressed as functions of generalized displacements ;

$$\{d_m\}_i = \begin{Bmatrix} u_i \\ v_i \\ \theta_{zi} \end{Bmatrix} = \begin{bmatrix} 1 & x_i & y_i & 0 & 0 & 0 & 0 & 0 & 0 \\ 0 & 0 & 0 & 1 & x_i & y_i & 0 & 0 & 0 \\ 0 & 0 & 0 & 0 & 0 & 0 & 1 & x_i & y_i \end{bmatrix} \cdot \begin{Bmatrix} A_1 \\ A_2 \\ A_3 \\ \vdots \\ A_9 \end{Bmatrix} \quad [4a]$$

$$\{d_b\}_i = \begin{Bmatrix} w_i \\ \theta_{xi} \\ \theta_{yi} \end{Bmatrix} = \begin{bmatrix} 1 & x_i & y_i & 0 & 0 & 0 & 0 & 0 & 0 \\ 0 & 0 & 0 & 1 & x_i & y_i & 0 & 0 & 0 \\ 0 & 0 & 0 & 0 & 0 & 0 & 1 & x_i & y_i \end{bmatrix} \cdot \begin{Bmatrix} A_{10} \\ A_{11} \\ A_{12} \\ \vdots \\ A_{18} \end{Bmatrix}$$

The unknown parameters are determined by minimizing the total potential of the element. With known displacement functions, the process of generating stifness coefficients is accomplished in the same way as described in reference [1].

(5) RESULTS AND DISCUSSIONS :

5.1 Loading case no. (1) :

Fig. [6] shows the principal stresses in the bracket. Fig. [7] & [8] show the distribution of the normal and shearing stresses respectively along the line of welding AB. The values of equivalent stresses for static and dynamic loading conditions are represented in fig.[9].

5.2 Loading case no. (2) :

In this case, where the load is lumped in extreme end of the folded plate, the shearing forces transmitted to the diaphragm (bracket), in its plane, are shown in fig. [10]. Fig.[11] shows the principal stresses in the bracket while fig.[12] & [13] show the distribution of the normal and shear stresses along the same line of welding AB. The resulting values of equivalent stresses for static and dynamic loading conditions are shown in fig. [14].

5.3 Allowable and ultimate stresses :

A) For the bracket material-Steel 37-according to DIN 1050 :

Allowable compressive and tensile stresses = 1600 Kg/cm2
Allowable shear stress = 900 Kg/cm2
Allowable equivalent stress
= 0.75 x yield stress = 1800 Kg/cm2
Yield stress = 2400 Kg/cm2
Ultimate stress = 3700 Kg/cm2

B) For the welding-under static loading-acording to DIN 4100 :

Allow. stress = 1350 Kg/cm2
Allow. principal stress = 1760 Kg/cm2

C) For the welding-under dynamic loading-according to Deutsche Bundesbahn Vorschrift DV 848 :

when $\frac{\sigma \text{ min.}}{\sigma \text{ max.}} = 0$ the allowable stresses are as follows : -

Allow. compressive	stresses	= 1000	Kg/cm2
Allow. tensile	stresses	= 900	Kg/cm2
Allow. Shear	stresses	= 1120	Kg/cm2
Allow. principal	stresses	= 1600	Kg/cm2

It should be noted that due to welding operation in thick plates initial stresses develop in the weld It should also be noted that due to the operational nature of the machine under consideration, the repitition of the load is very high, and accordingly the stress level is fluctuating from zero to its maximum value in short periods. For these reasons it is recommended to assume a factor of safty ranging from 1.2 to 1.3 to calculate the ultimate stresses in the weld.

(6) CONCLUSIONS :

From the results shown it can be concluded that :

- The internal stresses in the 70 mm thick bracket are within the allowable stresses.
- The internal stresses along the curved welded line AB of 2 x 12 mm fillet weld are higher than the yield stresses and reaches the ultimate stress values in the case of static loading. When considering the dynamic effects , secondary stresses and initial stresses it is expected that the failure along the weld line AB can take place under less critical cases of loading which represents the most common cases of loading under normal machine operation.

  Thus it is recommended to strengthen the welding by increasing the fillet weld. The new thickness can be calculated straight forward from the stresses shown.

REFERENCES :

[1] Szilard,E : "Theory and Analysis of Plates" , Prentice Hall , 1974.

[2] DIN 1050

[3] DIN 4100

[4] Deutsche Bundesbahn Vorschrift DV 848.

[5] Abdellah,G : Eine Finite-Element-Method zur Berechnung Beliebiger Faltwerke , Doctoral Dissertation T.U.Brauschweig , 1973.

[6] Timoshenko,S. and Goodier,I.N. : "Theory of Elasticity" 2nd ed., MC Graw-Hill Book Company,New York , 1951.

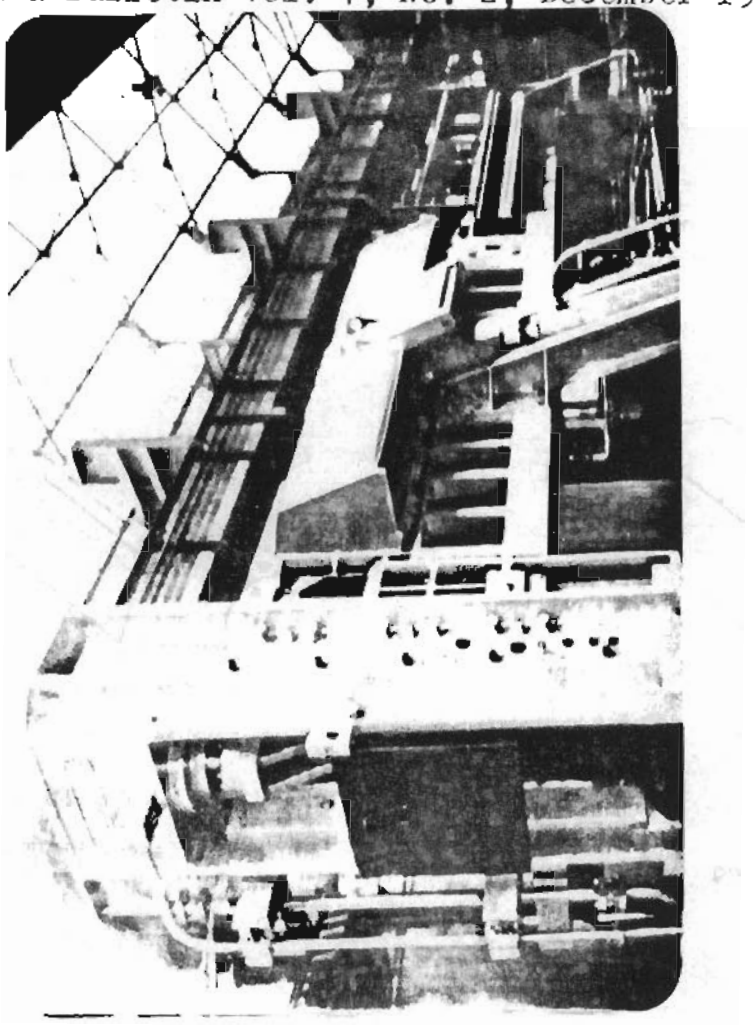

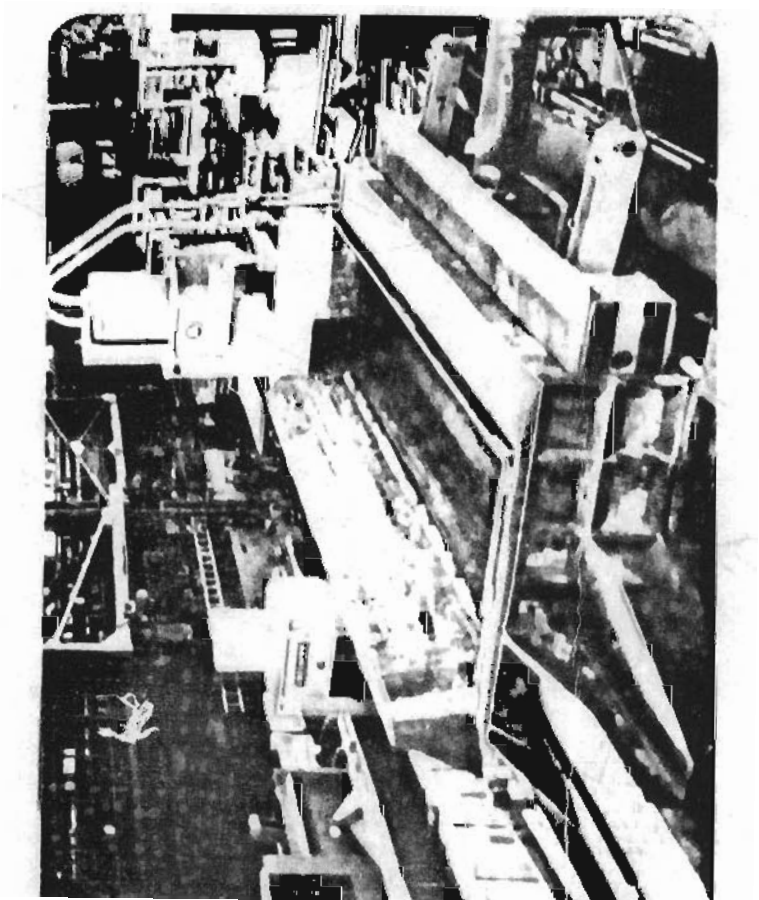

Fig (1) The Machine under consideration

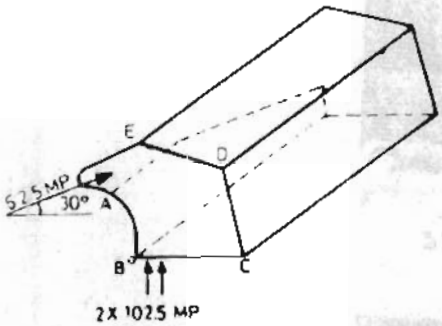

Fig. 2a

Case of loading N°1

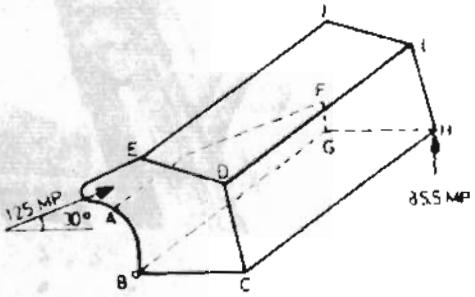

Fig. 2b

Case of loading N°: 2

Fig. 2: Press Cover

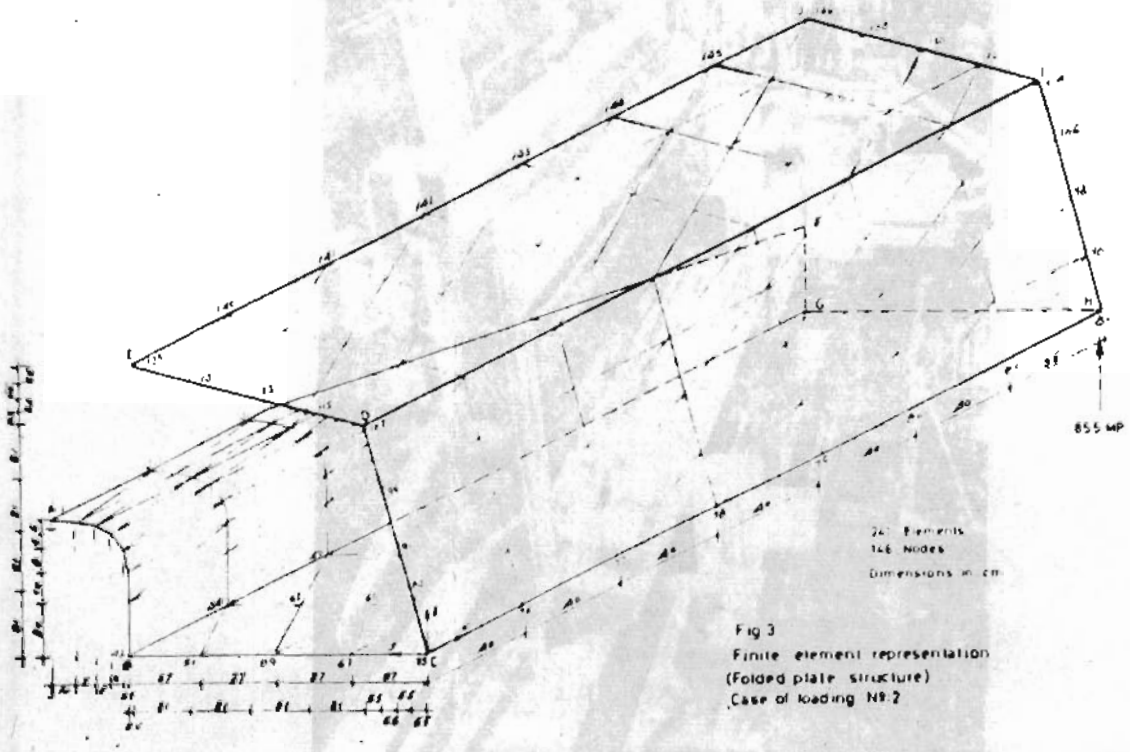

Fig 3

Finite element representation

(Folded plate structure)

Case of loading N°:2

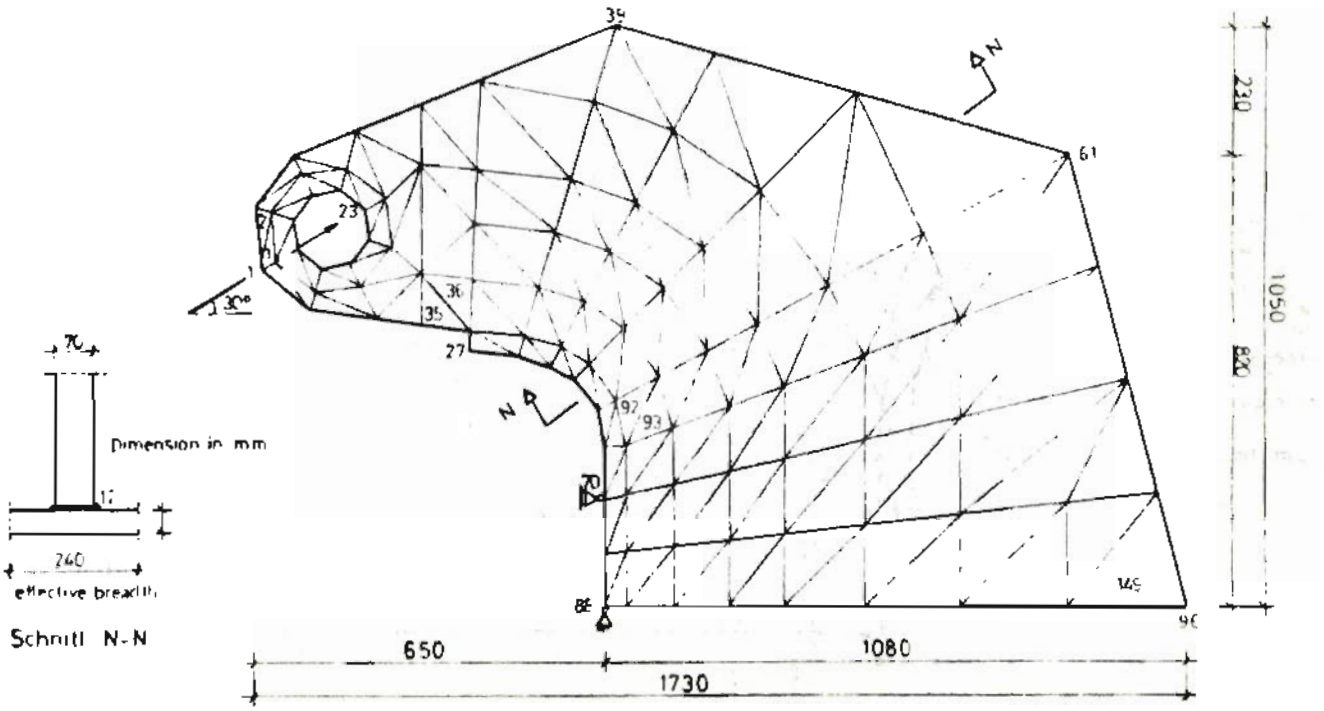

Fig 4 : Finite Element representation for
the main bracket
149 Element, 96 nodes

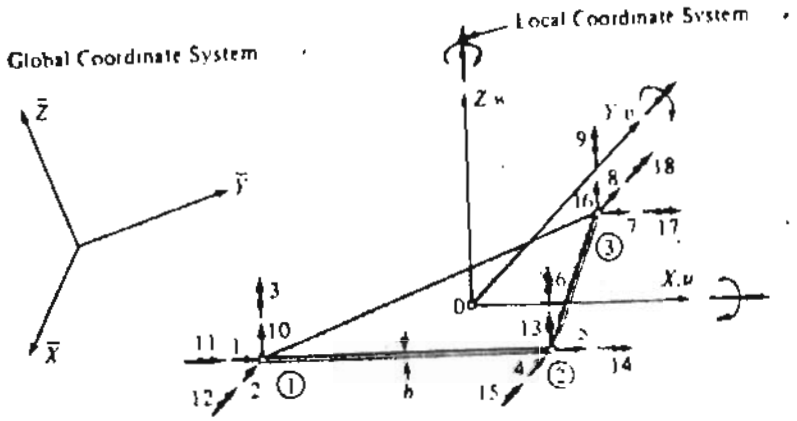

Fig. 5 : Triangular element.

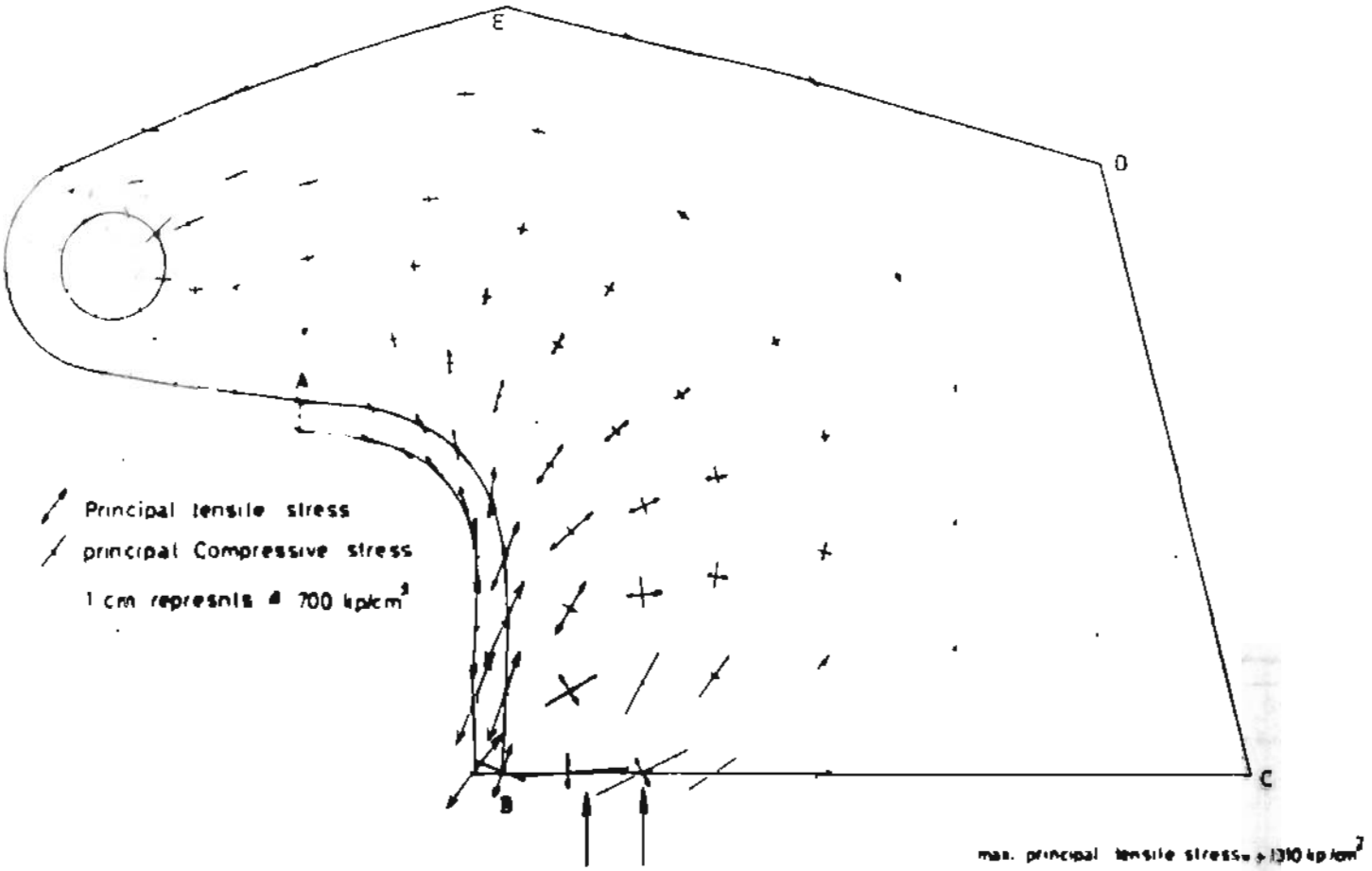

Fig. 6 :
Principal stresses in the 70 mm thick main bracket ABCDE - loading case N°:1

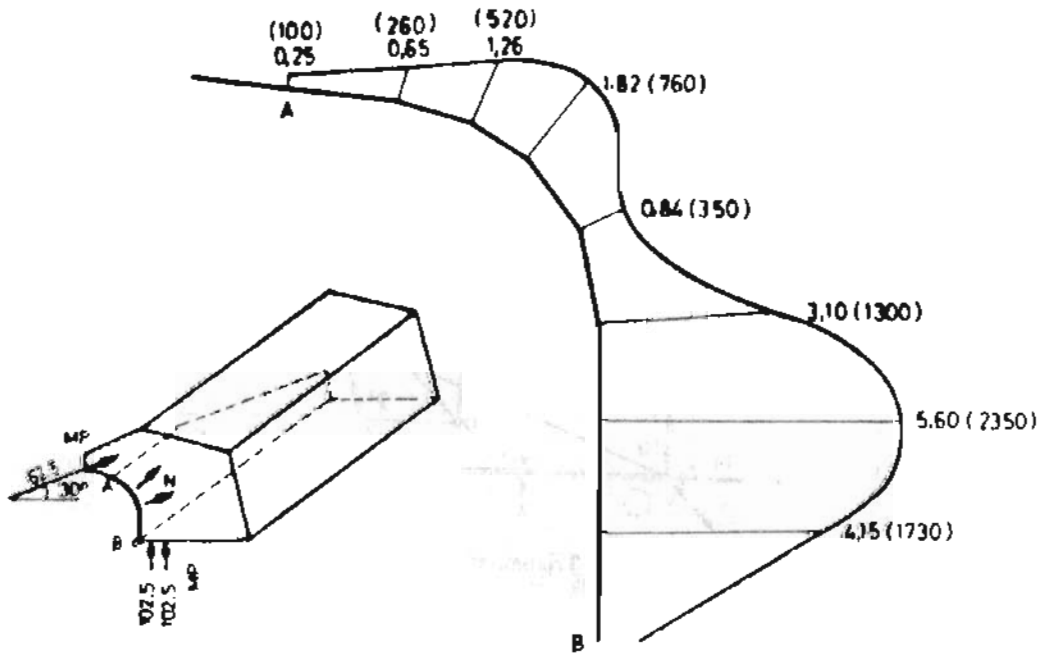

Fig.7 :

* Values in ( ) represent the corresponding stress

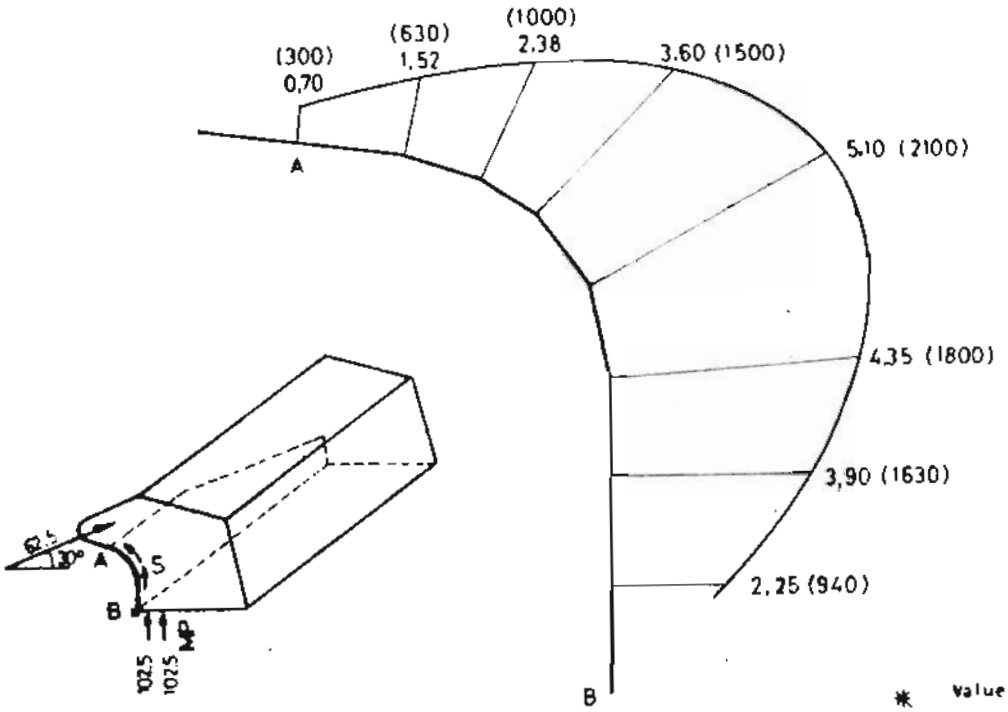

Fig.8: Distribution of Shearing forces (S in MP/cm) along the Welding seam A B resulting from loading case N8:1

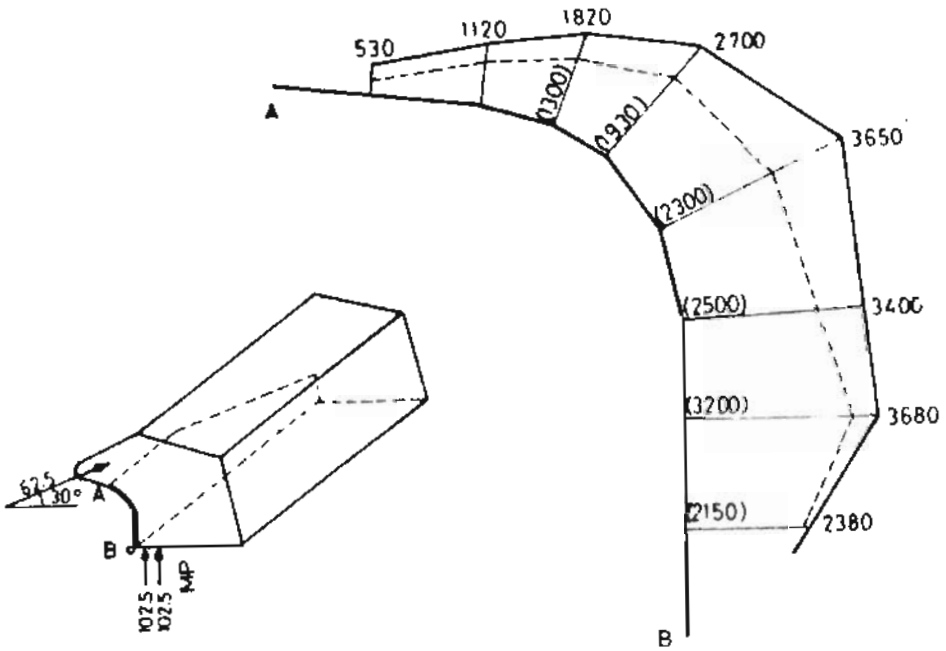

Fig.9 :

Distribution of the equivalent strese (Kp / cm^2) in the welding seam A.B resulting from loading case N8:1

——— Equivalent stress for static loading (distortion Energy hypothesis): $\sigma_v = \sqrt{\sigma^2 + 3\tau^2}$

- - - - - - Equivalent stress for dynamic loading

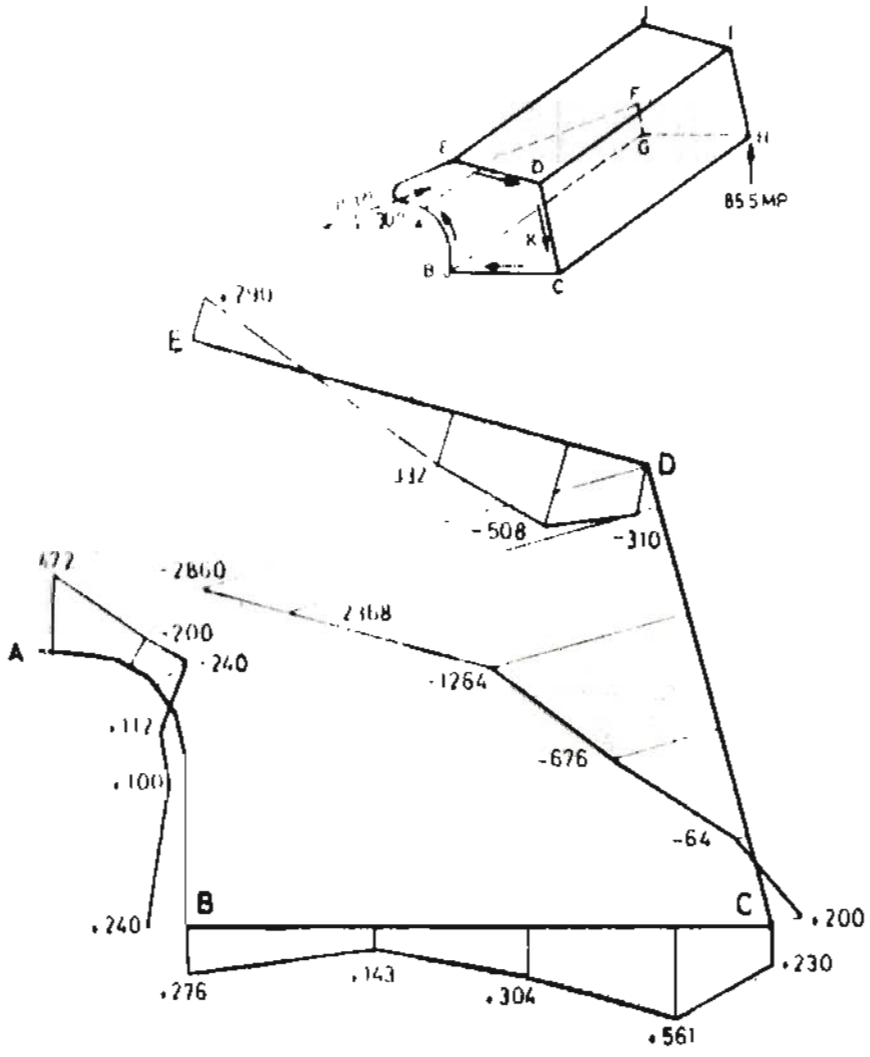

Fig 10:
Distribution of shearing forces (K in kp/cm²) along the boundaries of the main bracket (A-B-C-D-E) resulting from loading case N°.2

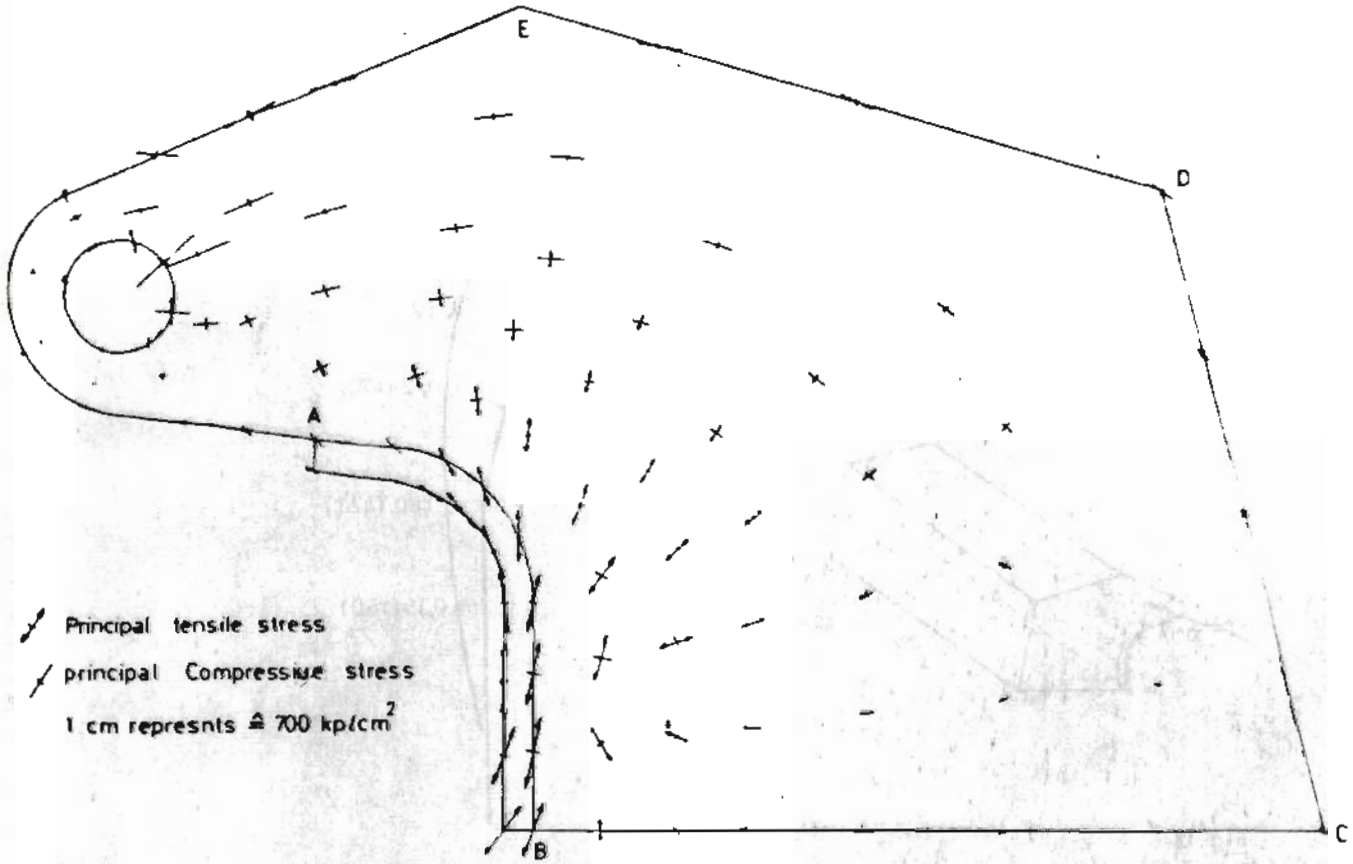

Fig.11 : Principal stresses in the 70 mm thick main bracket ABCDE loading case Nº:2

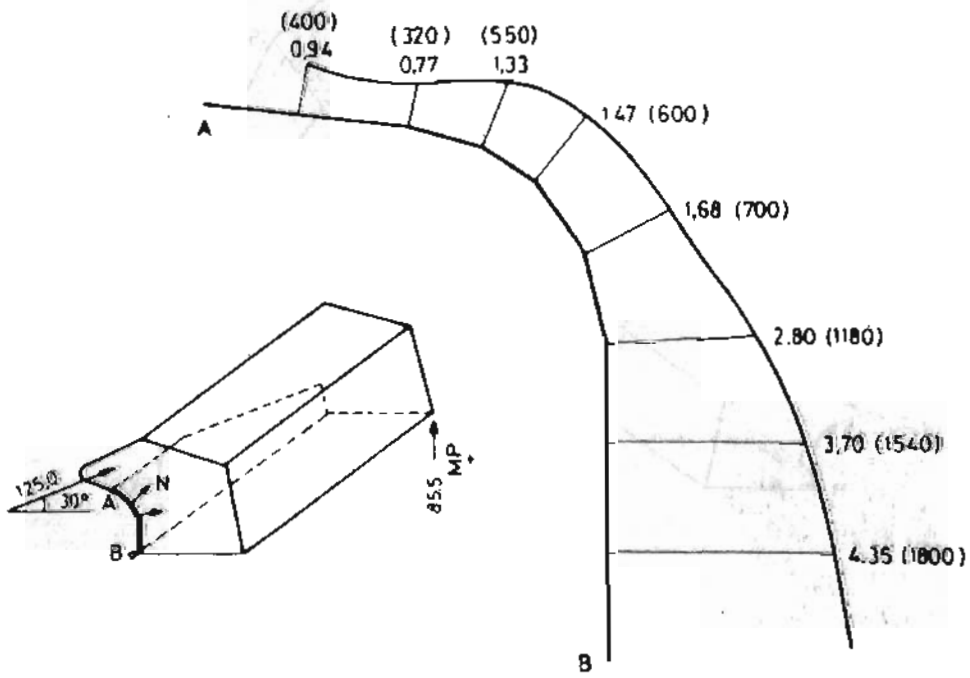

Fig.12 : Distribution of the normal forces (N in MP/cm) along the welding seam A B resulting from

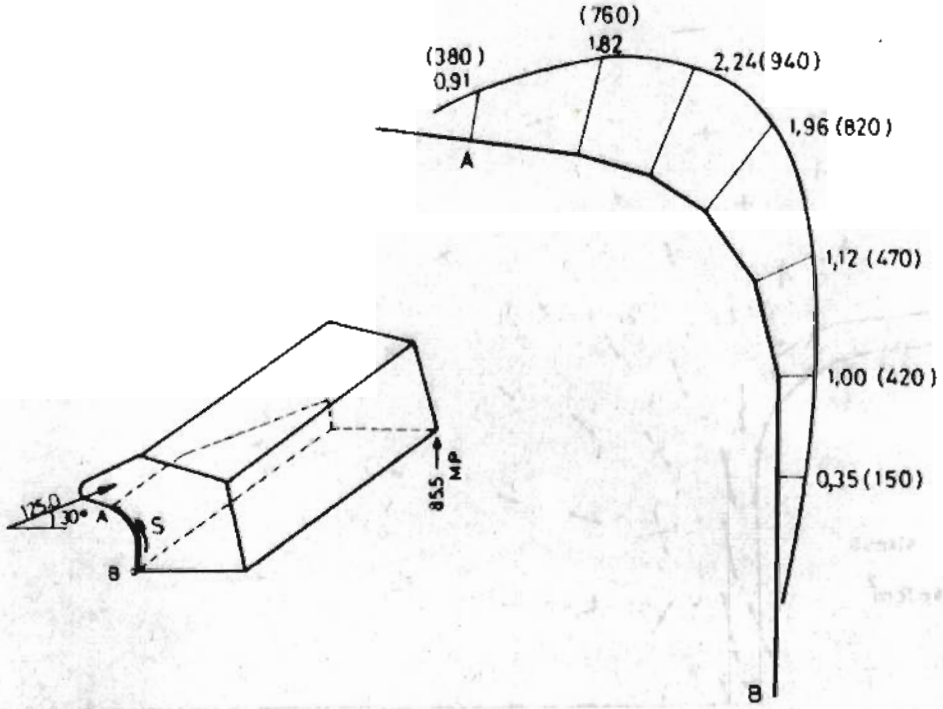

Fig. 13:
Distribution of shearing forces (S in MP/cm) along the welding seam A-B resulting from loading case Nº: 2

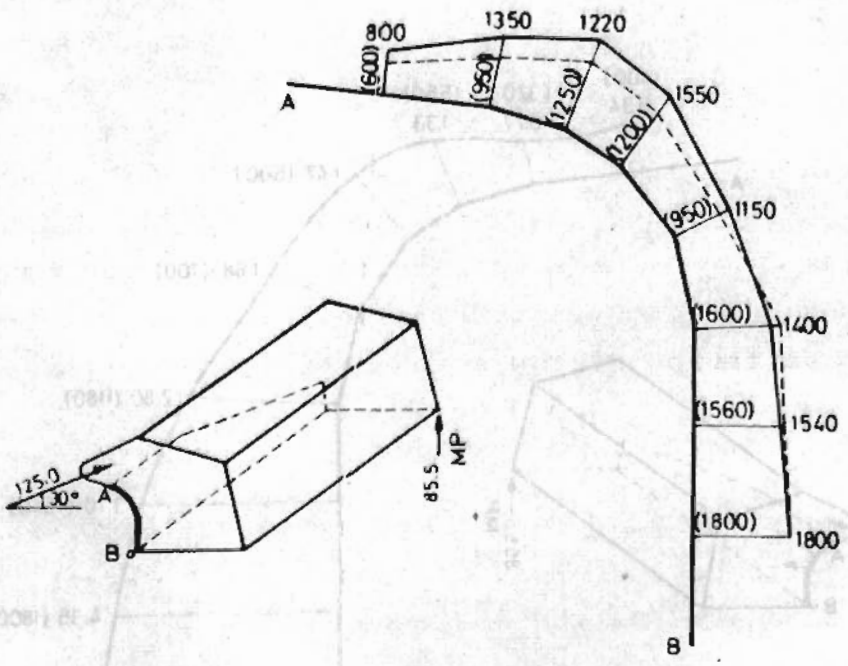

Fig 14:
Distribution of the equivalentstrese (Kp/cm²) in the welding seam A IB resulting from loading case Nº: 2
——— Equivalent stress for static loding
(distortion Energy hypothesis): $\sigma_v = \sqrt{\sigma^2 + 3\tau^2}$